Research Paper

Ubiquitin-specific Protease-7 Inhibition Impairs Tip60-dependent Foxp3 + T-regulatory Cell Function and Promotes Antitumor Immunity

Liqing Wang [a], Suresh Kumar [b], Satinder Dahiya [a], Feng Wang [b], Jian Wu [b], Kheng Newick [c], Rongxiang Han [a], Arabinda Samanta [a], Ulf H. Beier [d], Tatiana Akimova [a], Tricia R. Bhatti [a], Benjamin Nicholson [b,1], Mathew P. Kodrasov [b], Saket Agarwal [b], David E. Sterner [b], Wei Gu [e], Joseph Weinstock [b], Tauseef R. Butt [b], Steven M. Albelda [c], Wayne W. Hancock [a,*]

[a] Division of Transplant Immunology, Department of Pathology and Laboratory Medicine, Children's Hospital of Philadelphia and Perelman School of Medicine, University of Pennsylvania, Philadelphia, PA 19104, USA
[b] Progenra, Inc., Malvern, PA 19355, USA
[c] Pulmonary, Allergy & Critical Care Division, Perelman School of Medicine, University of Pennsylvania, Philadelphia PA19104, USA
[d] Division of Nephrology, Department of Pediatrics, Children's Hospital of Philadelphia and Perelman School of Medicine, University of Pennsylvania, Philadelphia, PA, USA19104, USA
[e] Institute for Cancer Genetics and Department of Pathology, College of Physicians and Surgeons, Columbia University, New York, NY 10032, USA

ARTICLE INFO

ABSTRACT

Foxp3 + T-regulatory (Treg) cells are known to suppress protective host immune responses to a wide variety of solid tumors, but their therapeutic targeting is largely restricted to their transient depletion or "secondary" modulation, e.g. using anti-CTLA-4 monoclonal antibody. Our ongoing studies of the post-translational modifications that regulate Foxp3 demonstrated that the histone/protein acetyltransferase, Tip60, plays a dominant role in promoting acetylation, dimerization and function in Treg cells. We now show that the ubiquitin-specific protease, Usp7, controls Treg function largely by stabilizing the expression and promoting the multimerization of Tip60 and Foxp3. Genetic or pharmacologic targeting of Usp7 impairs Foxp3 + Treg suppressive functions, while conventional T cell responses remain intact. As a result, pharmacologic inhibitors of Usp7 can limit tumor growth in immunocompetent mice, and promote the efficacy of antitumor vaccines and immune checkpoint therapy with anti-PD1 monoclonal antibody in murine models. Hence, pharmacologic therapy with Usp7 inhibitors may have an important role in future cancer immunotherapy.

1. Introduction

Lung cancer is the leading cause of death from cancer among men (28%) and women (26%), causing an estimated 158,040 deaths in the US in 2015 (American_Cancer_Society, 2015). The 5-year survival rate for all stages of lung cancer combined is currently only 17%, regardless of progress in surgical management, radiation, chemotherapy and ongoing developments in immunotherapy (American_Cancer_Society, 2015). Hence, there is a major need for new insights into the pathogenesis and management of lung cancer.

Tumors have distinctive properties of growth, invasion and metastasis (Hanahan and Weinberg, 2000), and the ability to evade immune destruction (Zitvogel et al., 2006). The latter is not because tumor cells lack antigenicity (Curiel, 2007). Rather, while tumor-infiltrating CD8 T cells are associated with improved clinical outcomes, accumulation of Foxp3 + T-regulatory (Treg) cells in tumors and/or draining lymph nodes has a negative prognostic effect for many solid tumors, including non-small cell lung cancer (O'Callaghan et al., 2015; Petersen et al., 2006; Woo et al., 2001). There is great interest in targeting inhibitory molecules expressed by immune cells, such as CTLA-4, PD1 and PD-L1 (Brahmer et al., 2012; Sharma et al., 2011; Topalian et al., 2012), and although some monoclonal antibodies (mAbs) to so-called immune checkpoints, e.g. anti-CTLA-4 mAb, probably bind Tregs and promote antibody-dependent cytolysis, there are no Treg-specific Abs (Pardoll, 2012). In experimental tumor models, beneficial strategies include depletion of Foxp3 + Tregs using CD4 or CD25 mAb, cyclophosphamide, IL-2-coupled toxin, or diphtheria-coupled toxin in so-called DEREG mice; use of agents that affect Treg development such as COX-2/PGE2, TGF-β, aromatase, STAT3 or p38 MAPK inhibitors, and TLR agonists; and antibodies that affect Treg recruitment (CCR4) or function (CTLA-4, PD-1, GITR, IL-10, TGF-β) (Beyer and Schultze, 2006; Curiel, 2007; Dougan and Dranoff, 2009; Dyck et al., 2016; Gallimore and Godkin, 2008; Gallimore and Simon, 2008; Ha, 2009; Ke et al., 2008; Nishikawa and Sakaguchi, 2010; Qin, 2009; Zitvogel et al., 2008).

* Corresponding author.
E-mail address: whancock@mail.med.upenn.edu (W.W. Hancock).
[1] Present address is Merck Research Laboratories, Boston, Massachusetts, USA.

However, none are Treg-specific, and all show only modest efficacy that may reflect co-targeting of activated effector T cells (Antony et al., 2005; Attia et al., 2005; Knutson et al., 2006). These various approaches also bring increased risks of autoimmunity (Dranoff, 2005) or inflammatory toxicity (Fietta et al., 2009), and have only transient effects (Powell et al., 2007).

In studies of the post-translational modifications of Foxp3, we have shown that modulation of Foxp3 protein acetylation by genetic or pharmacologic targeting of the histone/protein acetyltransferases (HATs), p300 and CBP, can dampen Treg suppressive function and promote anti-tumor immunity (Liu et al., 2013). These findings indicate the potential for pharmacologic regulation of Tregs without impairing host immune responses or inducing autoimmunity. In ongoing studies of additional members of the three main HAT families (GNAT, p300/CBP and MYST) (Roth et al., 2001), only deletion of the MYST family member, Tip60, led to lethal autoimmunity (Xiao et al., 2014). Indeed, the severity of autoimmunity seen in mice with conditional Treg deletion of *Tip60* was comparable to that in *Scurfy* mice that have a frame-shift mutation in the *Foxp3* gene.

We now report that both Tip60 and Foxp3 proteins are subject to ubiquitination and proteasomal degradation, whereas the actions of a deubiquitinating (DUB) enzyme, ubiquitin-specific protease, Usp7 (also known as HAUSP) (Cummins et al., 2004; Li et al., 2004), counteract these events and promote Tip60 and Foxp3 stability and, consequently, Treg suppressive function. Importantly, from a translational perspective, we further show that use of specific Usp7 inhibitors can, in a dose-dependent manner, promote anti-tumor immunity by dampening Treg activity while preserving key T effector cell functions, providing a new approach to cancer immunotherapy.

2. Materials and Methods

2.1. Animals

We purchased standard CD90.2+ C57BL/6 (B6), B6/CD90.1+, BALB/c, and B6/Rag1−/− mice (The Jackson Laboratory). CD4^{cre} mice (Lee et al., 2001), Foxp3$^{YFP-cre}$ mice (Rubtsov et al., 2008), Foxp3$^{eGFP-Cre-ERT2}$ mice (Rubtsov et al., 2010), Tip60$^{fl/fl}$ mice (Xiao et al., 2014), and Usp7$^{fl/fl}$ mice (Kon et al., 2011) were described previously. For tamoxifen induction of Foxp3$^{eGFP-Cre-ERT2}$, 40 mg of tamoxifen was dissolved in 100 μl ethanol, diluted by adding 900 μl of olive oil, and mice were gavaged with 200 μl tamoxifen emulsion per treatment. Mice were housed under pathogen-free conditions and used at 3–4 weeks of age, unless specified.

2.2. Antibodies and Plasmids

We purchased conjugated monoclonal antibodies (mAbs) for flow cytometry (BD Pharmingen), plus anti-Foxp3 mAb (FJK-16 s, eBioscience), and rabbit antibodies to β-actin, Usp7, p53 and Mdm2 (Cell Signaling), and Tip60 (Cell Signaling and Millipore). Flow cytometry was performed on a Cyan flow cytometer (Beckman Coulter), and data analyzed with FlowJo 8 software (Tree-Star). CD4$^+$YFP$^+$(Foxp3$^+$) and CD4$^+$YFP$^-$(Foxp3$^-$) cells were sorted from age- and sex-matched Foxp3$^{YFP-cre}$ or Foxp3$^{YFP-cre}$Usp7$^{fl/fl}$ mice using a FACS Aria cell sorter (BD Bioscience, UPenn Cell Sorting Facility). We purchased from Addgene plasmids expressing FLAG-tagged Foxp3 (pFLAG-Foxp3), pFLAG-Tip60, HA-tagged ubiquitin (pHA-Ub) and pUsp7, and 293 T cells were transiently transfected, as described (Xiao et al., 2014).

2.3. Hematology and Autoantibody Detection

Citrated blood samples were tested using an automated hematology analyzer modified and calibrated for mouse blood samples. Pooled sera from male *Usp7* −/− or WT mice were diluted 1:5 and incubated with cryosections from normal male and female C57BL/6 mice, washed in PBS, followed by goat anti-mouse IgG FITC-conjugated secondary antibodies (Jackson ImmunoResearch Laboratories, 1:200). In addition to pooled WT healthy sera, controls included incubation with secondary antibody alone. Pooled sera from NZB mice with known autoantibodies served as positive controls. If any autoantibodies were detected, serum from each mouse was re-analyzed separately.

2.4. Treg Suppression Assays

CD4 + CD25- T-effector (TE) and CD4 + CD25 + Treg cells were isolated from Foxp3$^{YFP-cre}$ or *Usp7* −/− mice using CD4 + CD25 + Treg isolation kits (130–091-041, Miltenyi Biotec). Cell Trace Violet-labeled or CFSE-labeled Teff cells (5×10^5) were stimulated with CD3 mAb (5 μg/ml) in the presence of 5×10^5 irradiated syngeneic T-cell depleted splenocytes (130-049-101, Miltenyi Biotec) and varying ratios of Tregs (Tao et al., 2007). After 72 h, proliferation of TE cells was determined by analysis of Cell Trace Violet dilution or CFSE dilution.

2.5. Treg Conversion from Conventional T Cells

CD4$^+$ YFP$^-$ TE cells isolated by cell sorting from Foxp3$^{YFP-cre}$ mice were incubated with CD3/CD28 beads (Invitrogen), IL-2 (10 U mL^{-1}) and TGF–β (2 ng/ml) for 3 days and analyzed by flow cytometry.

2.6. Homeostatic Proliferation

CD90.1$^+$CD4$^+$CD25$^-$ TE cells (1×10^6) were mixed with 0.5×10^6 CD4+ YFP+ Tregs sorted from FOXP3$^{YFP-cre}$ or *Usp7* −/− mice (CD90.2 +), and adoptively transferred to Rag1$^{-/-}$ mice (Tao et al., 2007). Spleen and lymph nodes were isolated at 7 days, and CD90.1$^+$ CD4$^+$ T-cells determined by flow cytometry. In separate studies of Treg survival, we undertook cell sorting and adoptively transferred 0.5×10^6 CD4 + YFP+ *Usp7* −/− or WT Tregs into syngeneic Rag1 −/− mice, and 4 weeks later, used flow cytometry to determine the numbers of each Treg population in peripheral lymph nodes and spleens.

2.7. Cardiac Transplantation

Intercrossed *Usp7*$^{fl/fl}$ and Foxp3$^{eGFP-Cre-ERT2}$ C57BL/6 mice were engrafted with fully MHC-disparate BALB/c cardiac allografts mice, and Treg-dependent allograft survival induced by costimulation blockade with i.v. injection of CD154 mAb (250 μg) plus 5×10^6 donor splenocytes (Tao et al., 2007). The effects of acute *Usp7* deletion in Foxp3 + Tregs of adult mice were assessed by treating recipients with tamoxifen, or carrier, at transplantation (n = 6/group). The effects of concomitant Usp7i therapy on costimulation blockade-induced cardiac allograft survival (BALB/c- > C57BL/6) in WT recipients (n = 6/group) was tested by daily injection of Usp7i (1 mg/kg/day, 14 days), or carrier alone, for 2 weeks from engraftment.

2.8. Quantitative PCR (qPCR)

RNA from Foxp3 + Treg or Foxp3- TE cells, freshly isolated from pooled lymph node and spleen samples, or isolated and activated with CD3/28 mAb-coated beads (Invitrogen), was obtained using RNeasy Kits (Qiagen). RNA was isolated from tumor samples using STAT-60 (Amsbio). cDNA was synthesized with TaqMan reverse transcription reagents (Applied Biosystems). qPCR was performed using TaqMan Universal PCR Master Mix (Applied Biosystems), and specific primers from Applied Biosystems, and gene expression data were normalized to 18S RNA.

2.9. Usp7 Reagents, DUB Biochemical Assays and Western Blotting

USP7i compounds, and assays of USP7 and total DUB activity were described previously (Chauhan et al., 2012; Weinstock et al., 2012). The UbiTest kit (LS catalog #UM411) was developed by LifeSensors. Immunoprecipitation and Western blotting were performed as previously described (Xiao et al., 2014).

2.10. ChIP Assays

DNA-chromatin complexes were prepared from 2×10^6 Tregs using EZ-Magna CHIP A Chromatin Immunoprecipitation Kits (17-408, Upstate), and genomic DNA immunoprecipitated using anti-Tip60 Ab or control IgG was probed by RT-PCR using primers for Foxp3 promoter: forward 5′-TTCCCATTCACATGGCAGGCTTCA-3′ and reverse 5′-TGAG ATAACAGGGCTCATGAGAAACC ACA-3′; Foxp3 CNS1 region: forward 5′-TAAAGGAGACTGGAAGCCAACATGG-3′ and reverse 5′-ATAGAAGA CATACACCACGGCG-3′; Foxp3 CN2 region: forward 5′-CAGAAAAA TCTGGCCAA GTT-3′ and reverse 5-‘AGGACCTGAATTGGATATGGT-3′; and Foxp3 CNS3 region: forward 5′-AAT GAATGAGACACAGAACT ATTAAGATGA-3′ and reverse 5′-CAGACGGTGCCACCATGAC-3′.

2.11. Microarrays

RNA was extracted with RNeasy kits (Qiagen) from Tregs isolated by cell-sorting of YFP+ cells, and RNA integrity and quantity were analyzed by photometry (DU640; Beckman-Coulter). Microarray experiments were performed with whole-mouse-genome oligoarrays (Mouse430a 2.0; Affymetrix), and array data analyzed with MAYDAY 2.12 (Battke et al., 2010). Array data were subjected to robust multiarray average normalization. Normalized data were used for calculating fold changes of genes that were increased or decreased in expression with the Student's t-test, and data with > 1.5–fold differential expression ($p < 0.05$ with Storey's FDR < 0.3) were included in the analysis. We assessed functional annotation clustering using the Database for Annotation, Visualization and Integrated Discovery (DAVID) (Huang da et al., 2009). Data underwent z-score transformation for display. Microarray data were deposited in NCBI Gene Expression Omnibus under accession code GSE72988.

2.12. Cell Lines and Tumor Models

TC1 cells were derived from mouse lung epithelial cells that were immortalized with HPV-16 E6 and E7, and transformed with the c-Ha-ras oncogene (Lin et al., 1996). The murine AE17.ova mesothelioma cell line was derived from mesothelioma cells developing in mice treated i.p. with asbestos, and then stably transduced with chicken ovalbumin (Jackaman et al., 2003). For tumor studies, each mouse was shaved on their right flank and injected s.c. with 1.2×10^6 TC1 or 2×10^6 AE17 tumor cells. For Usp7i experiments, mice received Usp7i or DMSO via Alzet pumps inserted 7 days after initial tumor injection. Tumor volume was determined by the formula: $(3.14 \times \text{long axis} \times \text{short axis} \times \text{short axis})/6$.

In Ad.E7 vaccination studies, 1×10^6 TC1 (E7$^+$) cells were injected subcutaneously into the right flanks of mice, and one week later, mice bearing TC1 flank tumors (~100 mm^3 in size) were either left untreated, or vaccinated subcutaneously in the left flank (contralateral to the tumor) with 1×10^9 plaque forming units (pfu) of Ad.E7 vector, as previously described (Haas et al., 2006). Three days following initial vaccination, mice received a booster vaccine of 1×10^9 pfu of Ad.E7 in the left flank and were thereafter untreated or received pumps delivering Usp7i (1 mg/kg/day). Tumor sizes were monitored twice/week, and antigen-specific T cells were identified using HPV-E7 tetramers, as described (Haas et al., 2006).

In PD-1 studies, mice with established TC-1 flank tumors were given i.p. injections of saline (control), anti-mouse PD-1 mAb (BioXcell)

(5 mg/kg/4 days), Usp7i (1 mg/kg/day, Alzet pump), or the combination of anti-PD1 mAb and Usp7i, and tumor sizes were monitored twice/week. In tumor studies, staff were blinded as to the contents of the Alzet pumps used in each experiment, and mice were followed until the size of tumors in control mice reached the size limit, or met additional limiting criteria, specified by our IACUC protocol.

2.13. Statistics

Data were analyzed by GraphPad Prism 5.0d. All normally distributed data were displayed as mean $\pm$ standard deviation (SD). Measurements between 2 groups were performed with a Student's t-test or Mann-Whitney U test. Groups of 3 or more were analyzed by one-way analysis of variance (ANOVA) or the Kruskal-Wallis test, with corresponding post-hoc tests (Tukey for ANOVA and Dunn's multiple comparison test for Kruskal-Wallis test). Survival analysis was calculated using Log rank (Mantel Cox) test.

2.14. Study Approval

Studies were approved by the Institutional Animal Care and Use Committee of the Children's Hospital of Philadelphia (IAC 13-000561 and 2014-1-1047).

3. Results

3.1. Developmental Deletion of Usp7 in Tregs Induces Lethal Systemic Autoimmunity

Our interest in Usp7 developed in several ways. First, recently published ChIP studies indicated that multiple *Usp* genes were targets of FOXP3 in human Tregs (Sadlon et al., 2010), suggesting a possible mechanism to control gene expression in Treg cells. Second, analysis of published databases showed that of various *Usp* genes, expression of *Usp7* in particular was markedly decreased by *Foxp3* ablation in murine Tregs (Fig. S1A). Third, both Foxp3 + Tregs and Foxp3- T-effector (Teff) cells, isolated from pooled lymph nodes and spleens, expressed Usp7 protein (Fig. S1B). Fourth, using immunoprecipitation studies, we found that Foxp3 and Usp7 proteins could co-associate (Fig. S1C). Fifth, a Dutch group reported that Usp7 regulated expression of Foxp3 in murine Tregs by promoting its deubiquitination and preventing its proteasomal degradation (van Loosdregt et al., 2013). Since none of these studies involved genetic deletion or the application of Usp7-specific pharmacologic inhibitors (Usp7i), we developed the current project to explore the significance of ubiquitination as a post-translational modification of potential significance as a therapeutic target in Foxp3 + Treg cells.

We conditionally deleted *Usp7* in murine Tregs by crossing *Usp7*$^{fl/fl}$ and *Foxp3*$^{YFP/Cre}$ mice (Fig. 1A). The resultant conditionally deleted (and hereafter termed *Usp7* −/−) mice were born at expected Mendelian ratios, but pups failed to thrive, showed progressive wasting by 3 weeks, and died by 4 weeks of life (Fig. 1B). The development of autoimmunity in these *Usp7*$^{-/-}$ mice was evidenced by: (i) thymic atrophy, lymphadenopathy and splenomegaly (Fig. 1C); (ii) pancytopenia with decreased hemoglobin and hematocrit levels (Fig. 1D); and (iii) extensive mononuclear cell infiltrates in lung, liver, pancreas and other tissues that were not present in age- and gender-matched controls (Fig. 1E, Table S1). In addition, in contrast to age- and gender-matched controls, 80% of *Usp7*$^{-/-}$ mice developed autoantibodies directed against gastric parietal cells, and 40% developed autoantibodies against pancreatic islet cells, endomysium, smooth muscle, keratin, and renal proximal tubular cell brush borders (Fig. 1F, Table S2). Hence, conditional deletion of *Usp7* within developing Foxp3 + Tregs led to severe autoimmunity and death of affected mice within 4 weeks of birth.
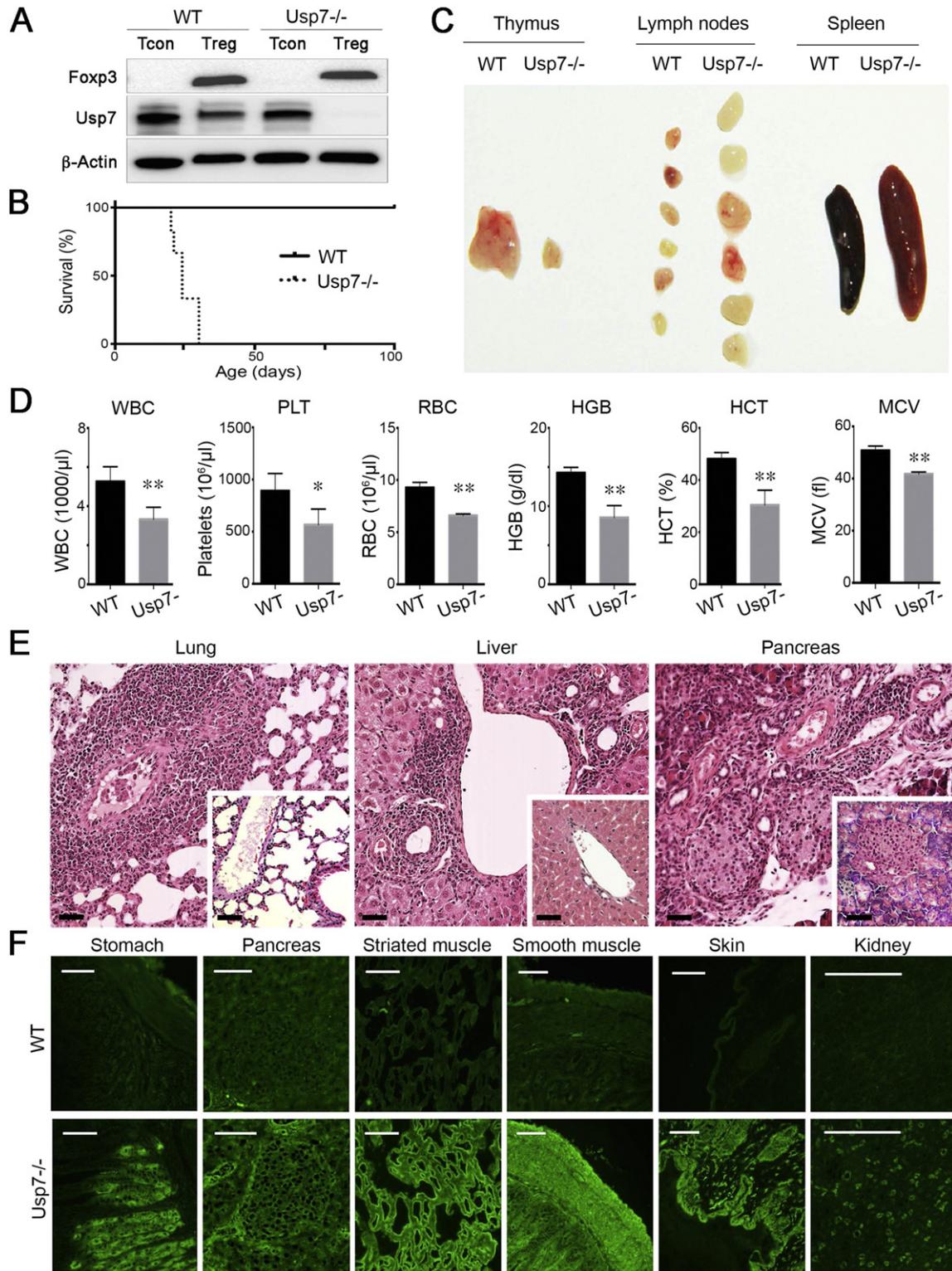
Fig. 1. Characterization of mice with conditional deletion of *Usp7* in their Foxp3 + Treg cells. Unless indicated, data are from male mice aged 3–4 weeks and are representative of 4 mice/ group. (A) Western blots showing deletion of Usp7 protein in *Usp7* −/− Foxp3 + Treg but not conventional T (Tcon) cells, following cell-sorting of YFP + and YFP- cells from USP7$^{fl/fl}$Foxp3^{cre} mice and Foxp3^{cre} controls. (B) Kaplan-Meier plot of the survival of *Usp7* −/− vs. WT mice (p < 0.01, 6 mice/group). (C) Thymus, spleen and lymph nodes from *Usp7* −/− versus WT mice. (D) Hematologic parameters (mean ± SD) in *Usp7* −/− versus WT mice, including white blood cell (WBC), platelet (PLT) and red blood cell (RBC) counts, plus hemoglobin (HGB), hematocrit (HCT) and mean corpuscular volumes (MCV), using blood samples from 6 mice/group; *p < 0.05, and **p < 0.01. (E) Representative histologic findings of dense mononuclear cell infiltrates in the lungs of *Usp7* −/− mice, periportal infiltration of the liver, and peri-islet infiltration of the pancreas; sections from age- and sex-matched littermate controls are shown as insets; scale-bars indicate 100 μ (F) Sera of *Usp7* −/− but not WT mice contained autoantibodies directed against gastric parietal cells of stomach, islet cells of pancreas, endomysium, smooth muscle cell membranes, keratin, and brush borders of renal proximal tubular cells; scale-bars indicate 100 μ

3.2. Effects of Usp7 Deletion on Foxp3 + Treg Development and Function

Conditional deletion of *Usp7* in Tregs did not markedly affect thymic CD4 or CD8 T cell development, but was associated with considerably increased T cell numbers and activation in lymph nodes and spleen (Fig. 2A, Fig. S2, p < 0.01), including increased CD69 + activated T cells and increased CD62L^{low}CD44^{high} effector/memory cells in both CD4 and CD8 T cell lineages (Fig. 2A, Fig. S2, p < 0.01). Deletion of *Usp7* did not appear to affect CD4 + Foxp3 + Treg development in the thymus, as the numbers of CD4 + YFP + or CD4 + Foxp3 + Tregs were comparable to those of littermate controls (Fig. 2B, Fig. S3). However, $Usp7^{-/-}$ Tregs displayed some very unusual properties. First, though the mean fluorescent intensity (MFI) of Foxp3 staining in Tregs from control vs. Usp7 −/− targeted mice was comparable (Fig. S3), the numbers of Treg cells in peripheral lymphoid tissues were significantly reduced (Fig. 2B, Fig. S3, p < 0.01), and $Usp7^{-/-}$ Tregs were more actively proliferating, even under basal conditions, than WT controls (Fig. S4, p < 0.05). Second, qPCR analysis showed that Tregs lacking *Usp7* actually had increased levels of Foxp3 compared to WT controls (p < 0.05), including following CD3/CD28 mAb-induced cell activation (p < 0.05) (Fig. S5A). Third, despite their increased Foxp3 transcription, $Usp7^{-/-}$ Tregs, in contrast to WT Tregs, produced the cytokines IL-2 and IFN-γ at baseline (p < 0.01), and their production of both cytokines was increased several hundred-fold upon cell activation (p < 0.01) (Fig. S5B). These data indicate that while Foxp3 + Tregs are produced in normal numbers in the thymus despite Usp7 deletion, and have increased Foxp3 transcription and apparently normal levels of Foxp3 protein, these cells are quite abnormal. In particular, they fail to suppress IL-2 production, which is a signature function of Foxp3 protein in normal Treg cells (Fontenot et al., 2005; Gavin et al., 2007), and they have reduced survival in the periphery despite increased proliferative rates.

We also analyzed the effects of *Usp7* deletion on the in vitro development of inducible Tregs (iTregs) using $Usp7^{-/-}$ conventional T cells, obtained by mating CD4^{cre} and Usp7$^{fl/fl}$ mice. These cells were activated and cultured for 3 days in the presence of TGF-β and IL-2. Compared to the iTreg conversion of WT T cells, iTreg development by cells lacking *Usp7* was reduced by >50% (p < 0.01) (Fig. 2C, Fig. S3). These findings suggest a markedly reduced capacity for extra-thymic Treg development as a result of peripheral conversion.

Microarray studies showed that *Usp7* deletion in Tregs affected the expression of several hundred genes (Fig. 2D), with decreased expression of many transcription factors important to Treg development and stability (Fig. S6), including the Foxp3 co-regulators *Eos* and *Gata1* (Fu et al., 2012; Rudra et al., 2012; Yang et al., 2016). *Usp7* deletion also increased Treg expression of genes associated with cell cycle, DNA damage response, apoptosis and glycolysis pathways (Fig. 2D, Fig. S7). The extensive changes in metabolic and pro-apoptotic gene expression in Usp7 −/− Tregs are consistent with their significantly decreased numbers in the periphery despite their concomitant increased proliferation.

As anticipated by the development of aggressive autoimmunity in $Usp7^{-/-}$ mice, the suppressive function of $Usp7^{-/-}$ Treg cells in vitro was markedly impaired (Fig. 2E). The rapid onset of autoimmunity and death in mice with conditional deletion of *Usp7* during normal development precluded in vivo studies of Treg function. Hence, to assess the importance of Usp7 in the Foxp3 + Treg cells of adult animals, we intercrossed Usp7$^{fl/fl}$ and Foxp3-$^{eGFP/Cre-ERT2}$ C57BL/6 mice. Their progeny developed normally and, as adults, displayed the anticipated normal Treg-dependent acceptance of BALB/c cardiac transplants when treated with CD154 mAb plus donor splenocyte transfusion (DST) (Hancock et al., 1998; Lee et al., 2005). However, this potent therapy for induction of Treg-dependent allograft tolerance was ineffective if corresponding allograft recipients were treated with tamoxifen, from the day of transplant, to deplete *Usp7* in their Tregs (Fig. S8), and acute rejection promptly ensued (Fig. 2F). Hence, *Usp7* deletion during thymic development, as well in adulthood when immune functions have fully developed, leads to profound effects on mature Foxp3 + Treg cells and disrupts their suppressive functions in vitro and in vivo.

3.3. Pharmacologic Inhibition of Usp7

To assess whether pharmacologic blockade of Usp7 could modulate normal Foxp3 + Treg cell function, we evaluated several highly selective small molecule inhibitors of Usp7 (Usp7i), including the parent compound P5091, and its derivative P0217564 (hereafter 564) (Chauhan et al., 2012; Weinstock et al., 2012), whose potencies and specificities are summarized in Table S3. We assayed the ability of each compound to target the active site of Usp7 and thereby prevent its interaction with an active site-directed probe, ubiquitin vinyl-methyl-ester (Ub-VME) (Boudreaux et al., 2010). In studies using full length Usp7, or just its catalytic domain, the pre-incubation of compound 564 prevented interaction of Usp7 and Ub-VME (data not shown). In studies in which Jurkat cells were incubated with 564 (10 μM) for 2 h and then washed free of compound, the Usp7i blocked >80% of Usp7 enzymatic activity, and in pulse chase studies maintained ~50% inhibition at 48 h, but did not affect global deubiquitinase activity (Fig. 3A). In the case of Foxp3 + Treg cells, the parent compound, P5091, and its derivatives, including 564 (all at 10 μM), had potent and long-lasting inhibitory effects on murine Treg function in vitro; 2 h of pre-treatment of Tregs, followed by their washing and use in 3-day suppression assays almost completely abrogated Treg function (Fig. 3B). These sustained inhibitory effects on Treg function were remarkable given the brief pre-incubation and are indicative of essentially irreversible Usp7 inhibition.

Reduced Treg function as a result of Usp7i treatment was consistent with the effects of gene targeting (Fig. 2), but the pharmacologic studies also suggested a more complex mechanism of action than initially anticipated. Thus, we detected a greater impact of Usp7i on a key HAT in Tregs, Tip60, which critically regulates Foxp3 dimerization and Treg function (Xiao et al., 2014), than on Foxp3 itself. First, cell-sorted Foxp3-$^{YFP+}$ Tregs isolated from WT or *Usp7* −/− mice had comparable levels of Foxp3 but markedly decreased Tip60 (Fig. 3C). Second, addition of compound 564, for 5 h, to 293T cells transfected with Foxp3 had negligible effects on expression of Foxp3 or endogenous Usp7, but downregulated expression of endogenous Tip60 (Fig. S9). Third, Western blots of Foxp3 + Treg cells activated for 2 h in vitro in the presence of 564 showed only negligible down-regulation of Foxp3 but a marked decrease in Tip60 expression (Fig. 3C). These data suggested that Usp7 might be especially important to the regulation of Tip60 expression in Treg cells.

To explore this further, we assessed the levels of Foxp3 expression in *Tip60* −/− vs. WT Tregs. *Tip60* −/− Tregs are present in only exceedingly low numbers following the conditional deletion of *Tip60* in Foxp3 + Tregs (Xiao et al., 2014), precluding obtaining a sufficient number of cells for Western blotting. However, flow cytometric staining, using Tregs pooled from several such mice, showed markedly decreased Foxp3 protein in *Tip60* −/− vs. WT Tregs, and qPCR analysis showed their lower expression of Foxp3 and Ctla4 mRNA (p < 0.01), but increased expression of IL-6 and IL-17 mRNA (p < 0.01), compared to WT Treg cells (Fig. 3D). Corresponding conventional T cells from these mice showed upregulated of Ctla4, IL-6 and IL-17 (p < 0.01), consistent with their activation in the presence of reduced Treg numbers. Lastly, ChIP studies showed that Tregs from conditionally deleted *Usp7* −/− mice had decreased recruitment of Tip60 to the conserved noncoding sequence-2 (CNS2) intron of the Foxp3 locus (Fig. 3E, p<0.01); this region is demethylated in mature Tregs and has a key role in maintaining Foxp3 expression and Treg lineage stability (Zheng et al., 2010). Consistent with data from conditionally targeted mice (Fig. 3C and Fig. S5), in ChIP studies of WT Foxp3 + Treg cells (Fig. S10), Usp7i treatment decreased recruitment of DNA polymerase II (Pol II) to the Tip60 promoter (p < 0.01), and decreased Foxp3 binding to the IL-2 promoter (p < 0.01). These data point to the importance of Tip60 to maintaining optimal Foxp3 expression in Treg cells.
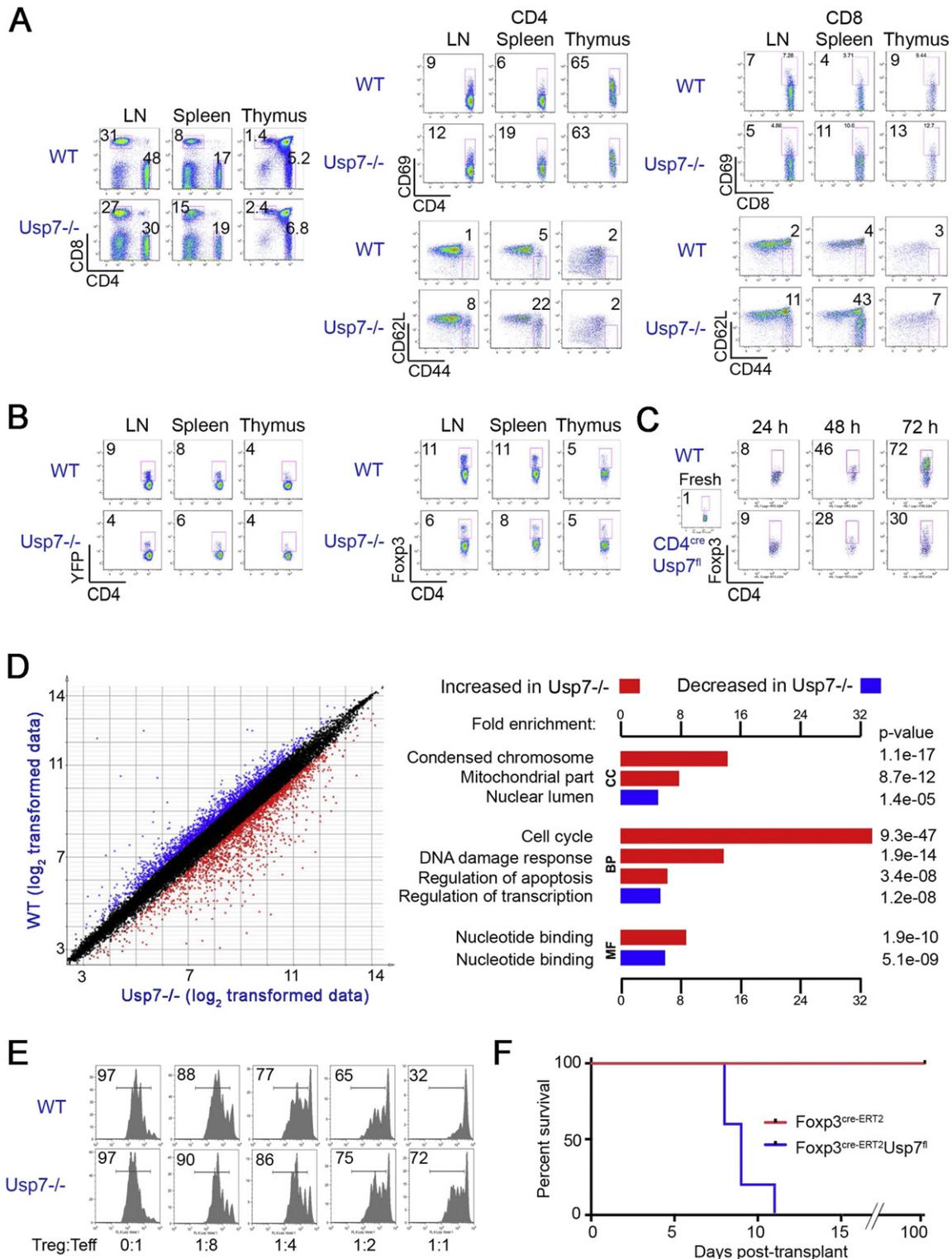
Fig. 2. Effects of *Usp7* deletion on Foxp3 + Treg development and function. Data are from 3 to 4 week old male mice, and are representative of results in 4 mice/group; additional summary graphs and statistical analyses are shown in Figs. S2–S7. (A) Generally normal proportions but increased activation of CD4 and CD8 cells (CD69 + CD44 + and CD62L^{low}CD44^{high} cells) in *Usp7* −/− versus WT mice. (B) Normal thymic Treg development but moderate decreases in YFP+ and Foxp3 + cells in peripheral lymphoid tissues of conditional *Usp7* −/− versus WT mice. (C) Marked impairment of iTreg development in a 3-day in vitro assay involving culture of WT vs. CD4^{cre}Usp7$^{fl/fl}$ T cells under activating conditions and in the presence of IL-2 plus TGF-β. (D) Microarray analysis: Left panel shows a scatterplot of log$_2$ transformed expression matrix data (means from 3/group) from YFP-sorted Foxp3^{cre} Tregs with or without conditional Usp7 deletion. Differential expression was determined by Student *t*-test p < 0.05 with >1.5-fold difference (log$_2$ 0.58), with red and blue representing genes up- and downregulated by Usp7 deletion, respectively. Data underwent z-transformation for display. Right panel shows enrichment scores of the up- or downregulated genes calculated using DAVID Functional Annotation Clustering. CC (cellular component), BP (biological process) and MF (molecular function) indicate gene ontology categories. (E) *Usp7* −/− vs. WT Tregs in a standard Treg suppression assay. (F) The long-term cardiac allograft acceptance in FOXP3$^{cre-ERT2}$Usp7$^{fl/fl}$ recipients promoted by CD154 mAb/DST therapy was abrogated by tamoxifen-induced depletion of *Usp7* in recipient Foxp3 + Treg cells (p < 0.01, n = 5/group).
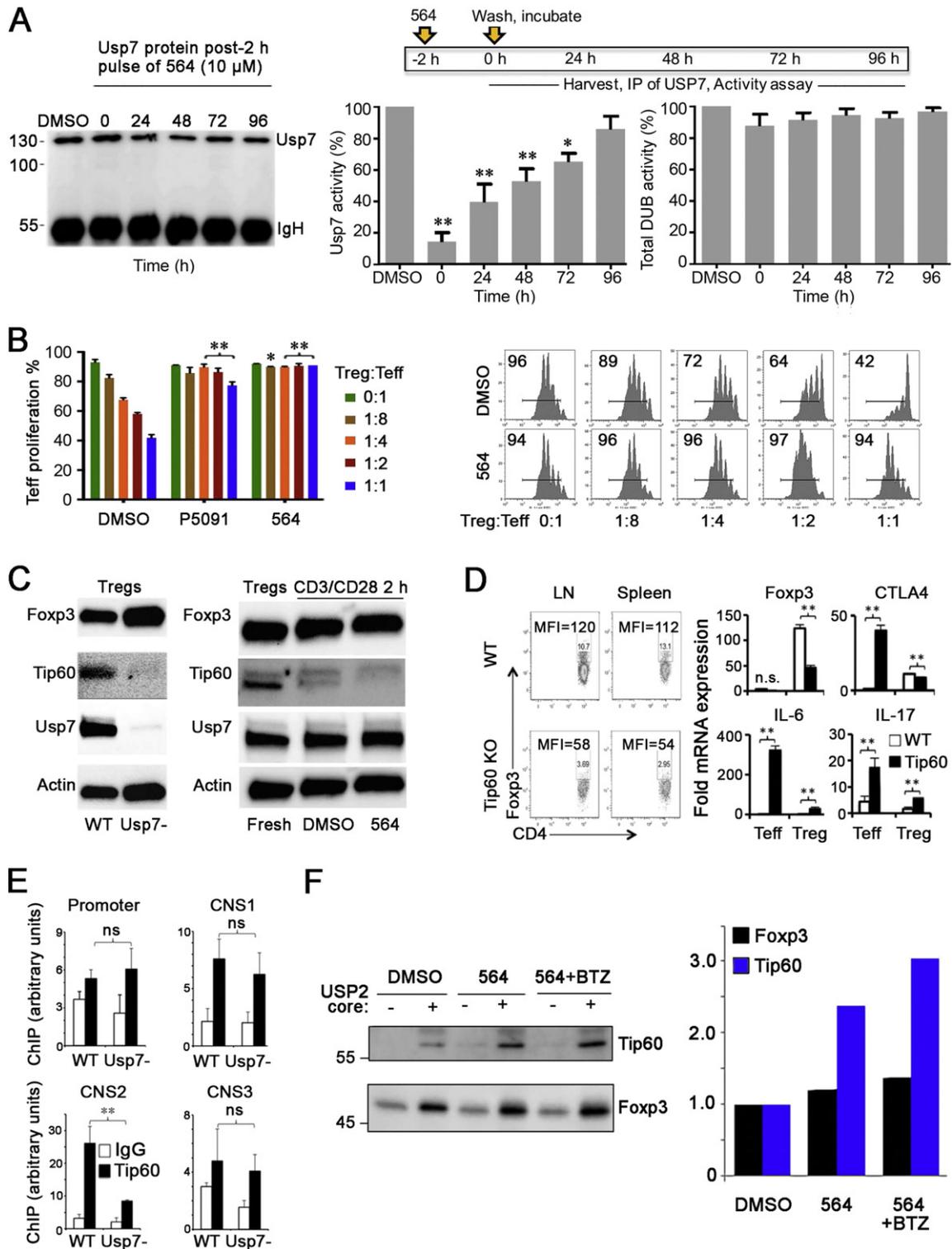
Fig. 3. In vitro effects of Usp7i compounds. (A) Jurkat cells were pulsed for 2 h with compound 564 (10 μM), washed free of compound and cultured for the periods indicated. Levels of Usp7 were serially monitored by Western blotting (left panel), in conjunction with assays of Usp7 (middle panel) or global DUB activity (right panel), expressed as a percentage of activity of corresponding DMSO-treated cells (mean ± SD); *p < 0.05 and p < 0.01 vs. DMSO-treated cells. (B) Murine Treg cells were pre-incubated with DMSO or Usp7i compounds for 2 h, washed and cultured for 3 days, at the ratios of Treg to CFSE-labeled Teff cells shown (mean ± SE of triplicate wells, *p < 0.05 and **p < 0.01 vs. DMSO-treated cells at the corresponding ratio); a representative result in which Tregs were pre-treated with compound 564 for 2 h is shown at right (inset figure indicates the proportion of proliferating cells in each well). (C) Western blot analysis of, in the left panel, lysates of cell-sorted Foxp3^{YFP+} Tregs from WT or $Usp7-/-$ mice, and right, levels of endogenous Foxp3, Tip60 and Usp7 in Foxp3+ Treg cells cultured under activating conditions for 2 h with or without the addition of compound 564, as shown. (D) Left panel shows mean fluorescent intensity (MFI) levels of Foxp3 in WT or conditional Tip60−/− Treg cells isolated from corresponding LN and spleen samples (representative of 4 mice/group). Right panels show qPCR data (mean ± SD, 4/group, **p < 0.01) of Foxp3, Ctla4, IL-6 and IL-17 mRNA levels using Teff and Treg cells isolated from WT or conditional $Tip60-/-$ mice. (E) ChIP studies assessing the levels of Tip60 at the Foxp3 promoter and CNS1, CNS2 and CNS3 sites in WT and conditionally deleted $Usp7-/-$ Tregs (mean ± SD, 4/group, **p < 0.01). (F) Murine WT Tregs were incubated with DMSO alone, 564 (10 μM), or 564 plus proteasome inhibitor (Bortezomib, BTZ) for 2 h, washed, lysed, subjected to TUBE pull-downs, and ubiquitinated substrates eluted and treated with Usp2 to separate ubiquitin from substrate; proteins were then analyzed by Western blotting. Data are expressed at right as fold change compared to using DMSO alone, and are representative of 3 separate experiments.

We next tested whether Usp7 regulated the ubiquitination and proteasomal degradation of Tip60 and Foxp3, beginning with 293T cells transfected with Foxp3, Tip60 and Usp7 (Fig. S11). Both proteins were readily ubiquitinated, and ubiquitination was markedly suppressed by co-transfection of Usp7, whereas Usp7i treatment promoted Foxp3 and Tip60 ubiquitination (Fig. S11). In native gels, Foxp3 was mainly expressed as dimers in 293T cells transfected with Foxp3 alone, whereas addition of tagged Usp7 resulted in expression of Foxp3 monomers, as well markedly increased dimer and oligomer formation (Fig. S12, left panel). Treatment with Usp7i decreased Foxp3 monomers, dimers and oligomers in transfected 293T cells (Fig. S12, right panel). To assess whether Usp7i treatment also promoted ubiquitination of Foxp3 in WT Treg cells, we studied Tregs cultured in the presence of 564 and a proteasome inhibitor (MG132). Usp7i treatment increased the levels of ubiquitinated Foxp3 in Tregs, and detection was markedly enhanced by inclusion of MG132 to prevent the very rapid proteasomal degradation of ubiquitinated Foxp3 (Fig. S13). Analysis using native gels showed that Usp7i treatment largely abrogated detection of native Foxp3 monomers and dimers (Fig. S14, left), whereas oligomers and high MW complexes of heavily ubiquitinated Foxp3 were detected in the presence of increasing concentrations of MG132 (Fig. S14, right). These data implicate proteasomal turnover of Foxp3 and Tip60 rather than their ubiquitin-dependent lysosomal degradation (Du et al., 2013). Hence, Usp7 can promote assembly of higher order complexes of Foxp3, including formation of Foxp3 dimers that are essential for optimal Foxp3 binding to DNA in Treg cells, whereas Usp7i treatment can disrupt assembly of such complexes. These actions likely reflect the effects of Usp7 targeting on Tip60 expression, since Tip60, as shown, is subject to Usp7-regulated deubiquitination, and normally functions to promote Foxp3 acetylation and dimerization (Xiao et al., 2014).

To further assess test the relative effects of Usp7i compound on ubiquitination of Treg-associated Foxp3 and Tip60, we used a UbiTest assay in which ubiquitinated proteins are pulled down using agarose coupled to Tandem Ubiquitin Binding Entities (TUBE), followed by their elution and treatment with a broadly acting DUB enzyme, Usp2, to remove ubiquitin from substrate proteins. Using this DUB-assisted ubiquitination detection assay, we found that whereas Tregs incubated with 564 for 2 h in vitro showed only a modest increase in levels of ubiquitinated Foxp3, the levels of ubiquitinated Tip60 were increased by about 3-fold (Fig. 3F). Collectively, these data indicate that pharmacologic inhibition of Usp7 can markedly curtail Treg function, likely through mechanisms that involve Tip60 rather than simply via direct actions on Foxp3 alone.

3.4. In Vivo Effects of Usp7 Targeting on Foxp3 + Tregs

To assess the in vivo effects of Usp7i, we first injected mice daily for 5 days with Usp7i and isolated their Treg and Teff cells for Western blotting. The administration of Usp7i in vivo led to modestly decreased Foxp3 protein and increased Ub-Foxp3 in Tregs (Fig. 4A). However, Usp7i treatment resulted in markedly impaired Treg suppressive function ($p < 0.01$), and also increased the resistance of Usp7i-treated Teff cells to suppression by untreated WT Tregs ($p < 0.05$) (Fig. 4B, Fig. S15). To assess the direct effects of brief exposure of T cells to Usp7i in vivo, we injected normal mice with compound 564 or diluted DMSO carrier, and 2 h later, Treg and Teff cells were isolated for biochemical studies. Brief Usp7i exposure had modest effects on the levels of Foxp3 protein in Tregs, but markedly decreased concomitant Tip60 protein expression, whereas levels of Tip60 in Teff cells were less affected (Fig. 4C). In addition, extracts of the harvested cells were treated with HA-Ub-VME that binds to the active site of Usp7, and analyzed using SDS-PAGE. The in vivo binding of compound 564 to the active site of Usp7 blocked the interaction of Usp7 with VME substrate, revealing broadly equivalent interactions of compound 564

and Usp7 enzyme in both Treg and Teff cells (Fig. 4D), whereas global DUB activity in either cell population was unaffected (Fig. S16).

We next tested the effects of Usp7 targeting using 3 in vivo models. The first model assessed the effects of Usp7 deletion on Treg survival by undertaking the adoptive transfer of conditionally deleted Usp7 −/− or WT Tregs into syngeneic immunodeficient (C57BL/6 Rag1 −/−) mice. The numbers of Usp7 −/− Tregs recovered from lymphoid tissues after 4 weeks were markedly decreased compared to the numbers of correspondingly transferred WT Tregs, suggesting that Usp7 deletion impaired Treg survival in vivo (Fig. 4E), consistent with the reduced numbers of Tregs found in Usp7 −/− mice (Fig. 2B and Fig. S3). Preferential effects of Usp7i on Treg vs. Teff function were confirmed in 2 subsequent models. Next, in a 7-day model of homeostatic proliferation in immunodeficient mice, the treatment of Tregs with a Usp7i compound prior to their adoptive transfer markedly impaired their ability to suppress proliferation of co-transferred Teff cells, as compared to Tregs exposed to carrier alone (Fig. 4F). Third, treatment with Usp7i therapy for 2 weeks from the day of cardiac engraftment blocked the Treg-dependent permanent allograft survival (BALB/c- > C57BL/6) achieved in recipients treated with CD154 mAb plus donor splenocyte transfusion (DST) (Fig. 4G). These studies point to the potential for Usp7 targeting with selective small molecule inhibitors to impair Treg functions, likely through effects on Tip60 and/or Foxp3, while preserving important protective host T cell responses.

3.5. Effects of Usp7i on Tumor Growth in Syngeneic Mice

Turning to several tumor models, we first tested the ability of Usp7i compounds to differentially impair Treg vs. Teff cell functions in cancer, using syngeneic C57BL/6 mice bearing human papilloma virus (HPV)-E7 + TC1 lung adenocarcinoma cells, as growth of TC1 cells in these mice is Foxp3+ Treg-dependent (Liu et al., 2013). Therapy with Usp7i, 564, at 1.0 or 6.0 mg/kg/day significantly decreased the growth of TC1 tumors in WT mice (Fig. 5A), but had no effect on tumor growth when tested at the same dosing in immunodeficient mice (Fig. 5B). For mechanistic studies, additional groups were treated in the same manner and tumor samples were collected at 6 days after onset of USP7i therapy, when both 1.0 and 6.0 mg/kg/day of compound 564 had inhibitory effects on tumor growth (Fig. S17). At this point, the higher dose (6 mg/kg/day) decreased intratumoral accumulation of FOXP3 + Treg cells ($p < 0.01$, Fig. 5C), and both Usp7i concentrations (1 and 6 mg/kg/day) increased tumor infiltration by CD8 T cells ($p < 0.05$, Fig. 5D), including tumor-specific tetramer-positive CD8 T cells recognizing HPV-E7 ($p < 0.05$, Fig. 5E), and IFN-γ-producing CD8 T cells ($p < 0.01$ Fig. 5F); representative flow plots are shown in Fig. S18.

Usp7i compounds were next tested using AE.17 tumor cells, a second model in which tumor growth is Foxp3+ Treg-dependent (Liu et al., 2013). As with TC1 tumors, growth of AE.17 mesothelioma cells was impaired by Usp7i administration in syngeneic WT C57BL/6 mice (Fig. 6A), but Usp7i had no effect on tumor growth when tested in syngeneic immunodeficient mice (Fig. S19A). The lack of any significant direct effect of Usp7i on growth of TC1 or AE.17 cells in immunodeficient mice may reflect their lower levels of Usp7 than in the multiple myeloma (MM1.S) cells used in a prior publication showing inhibitory effects of Usp7i on tumor growth (Chauhan et al., 2012), as well as their low levels of p53 and Mdm2 that are classic targets of Usp7 (Fig. S19B). Together with the TC1 data, these findings show that the inhibitory effects of Usp7i on tumor growth result from immune actions, in particular, the differential effects of the Usp7i compounds on Treg vs. Teff cells in these models.

To assess the effects of Usp7i administration in combination with other anti-tumor therapies, we began by testing whether Usp7i use could potentiate tumor vaccine therapy. TC1 tumor cells, which express E7 derived from HPV, were implanted into WT B6 mice and on day 6 post-injection, mice were immunized with an adenovirus expressing HPV-E6 and -E7 proteins and also received Alzet pumps delivering
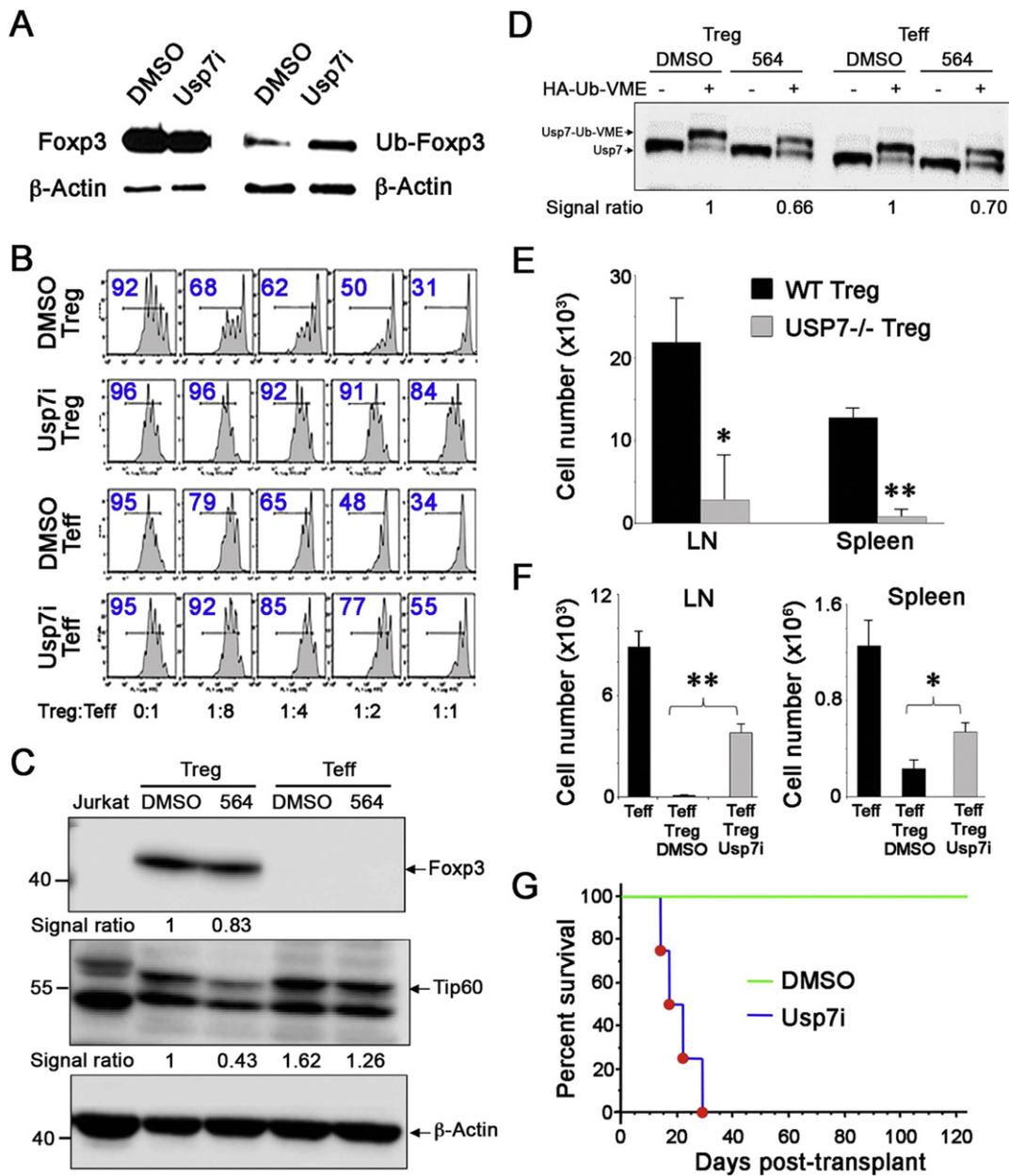
Fig. 4. In vivo effects of Usp7i compounds. For panels (A, B), mice were injected with Usp7i (10 mg/kg/day, i.p.) for 5 days or DMSO alone (5 mice/group). (A) Treg cells isolated from Usp7i-treated mice showed modestly decreased Foxp3 protein but increased Ub-Foxp3 compared to use of DMSO alone. (B) Treg cells isolated from Usp7i-treated mice showed markedly impaired Treg suppressive function compared to DMSO-treated Treg controls (upper 2 rows). Usp7i therapy also impaired Teff cell responses to Treg suppression, as shown using Teff cells from Usp7i or DMSO-treated mice and fresh, untreated Treg cells (lower 2 rows). Summary graphs and statistical analyses are shown in Fig. S15. (C) Western blots showing how a bolus injection of Usp7i 24 h beforehand decreased Tip60 protein to a greater extent than Foxp3 protein in murine Treg cells (panel shows ratios of data for 564 vs. DMS0). (D) Western blot analysis of the same cells as used in the previous panel, indicating that Usp7i compound bound to both Treg and Teff cells and decreased the interaction of Usp7 with HA-Ub-VME substrate (signal ratios shown below). (E) The effect of conditional *Usp7* deletion on the survival of Tregs in vivo was assessed by the adoptive transfer of Thy1.1 + Teff (5×10^5) plus WT Treg or *Usp7* −/− Treg (1×10^5) cells into immunodeficient (Rag1 −/−) hosts, and harvesting LN and spleen samples at 1 month post-transfer for flow cytometric quantitation (n = 4/group, **p < 0.01). (F) The effects of Usp7i on Treg cell inhibition of the homeostatic proliferation on Teff cells in vivo was assessed by pre-incubation of murine Tregs (5×10^5) with Usp7i (5 μM) or DMSO alone for 2 h, followed by their injection into Rag −/− mice, along with 1×10^6 Teff cells, and harvest of LN and spleen samples 7 days later (n = 4/group, *p < 0.5, **p < 0.01). (G) Use of CD154 mAb plus DST induces permanent cardiac allograft survival in DMSO-treated hosts (BALB/c- > C57BL/6) whereas daily injection of Usp7i (1 mg/kg/day, 14 days) from the time of engraftment restored acute allograft rejection (p < 0.01, n = 6/group).

Usp7i or DMSO carrier. The combination of Ad.E7 and Usp7i was significantly more effective than either agent alone in limiting TC1 tumor growth (Fig. 6B). Combination therapy significantly increased the numbers of tumor-specific CD8 + tumor infiltrating lymphocytes (Fig. 6C, with representative flow plots shown in Fig. S20) and their production of IFN-γ (Fig. 6D), while decreasing accumulation of intratumoral Foxp3 + Treg cells (Fig. 6E). Usp7i therapy also added significant therapeutic activity when used in combination with anti-PD-1 mAb therapy in mice bearing TC1 lung tumors (Fig. 6F). Collectively, these studies show that Usp7i therapy has significant benefits when used as

monotherapy in tumor models in syngeneic hosts, as well as when employed in combination with other forms of immunotherapy to promote antitumor immunity.

4. Discussion

Studies of HDAC and HAT enzymes in Foxp3 + Treg cells show that their regulation of the acetylation of lysine residues within Foxp3 protein is important to the development and maintenance of Treg cells (Li et al., 2007; Liu et al., 2014; Liu et al., 2012; Tao et al., 2007;
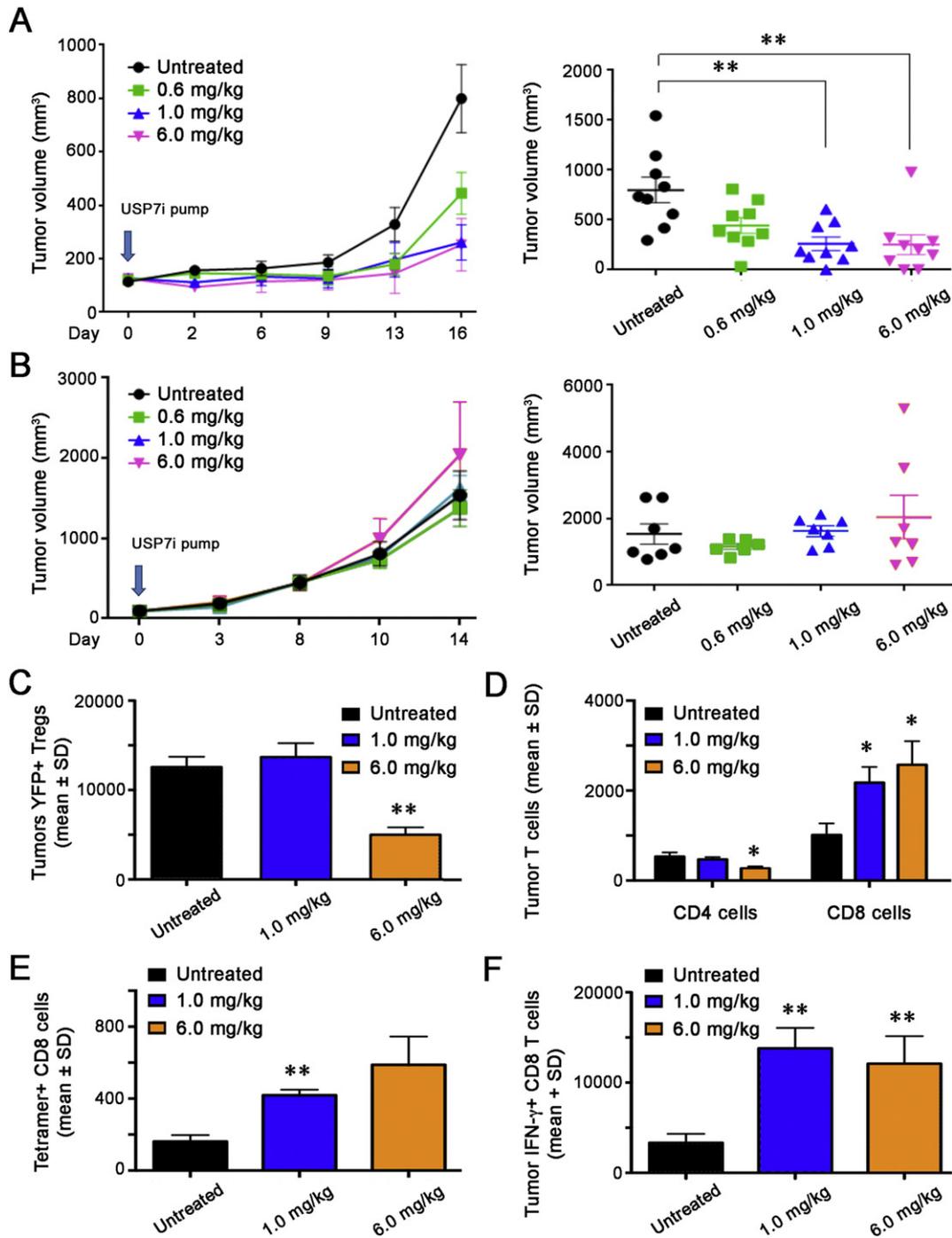
Fig. 5. Effects of Usp7i monotherapy on host anti-tumor immune responses. TC1 lung adenocarcinoma cells (1.2×10^6) were injected s.c., and once tumor volumes had reached ~150 mm³, mice (8–10 mice/group) were randomized and received either no therapy, or Usp7i (compound 564) at 0.6, 1.0 or 6 mg/kg/day, via 14-day Alzet pumps. (A) Inhibitory effects of Usp7i on tumor growth in syngeneic immunocompetent C57BL/6 mice; left panel shows serial tumor volumes (mean ± SD), and right panel shows individual tumor plots at day 16 of Usp7i therapy (**$p < 0.01$). (B) Lack of effects of Usp7i on tumor growth in immunodeficient Rag1 −/− C57BL/6 mice; left panel shows serial tumor volumes (mean ± SD), and right panel shows individual tumor plots at day 14 of Usp7i therapy. Panels (C–F) were obtained from tumors in additional mice that were harvested at day 6 of Usp7i therapy (see Fig. S11), and show data from 4 mice/group (mean ± SD), *$p < 0.05$, $p < 0.01$). (C) Inhibitory effects of Usp7i on numbers of intratumoral YFP + Foxp3 + Treg cells. (D) Usp7i administration impaired CD4 T cell accumulation but promoted intratumoral CD8 T cell recruitment. (E) Usp7i therapy increased tumor-specific tetramer-positive CD8 T cells. (F) Usp7i therapy increased intratumoral production of IFN-γ by CD8 T cells.

Wang et al., 2015). One HAT, Tip60, is especially important by promoting the acetylation-dependent dimerization of Foxp3 (Song et al., 2012; Xiao et al., 2014). This is an irreplaceable function of Tip60, since its conditional deletion in Tregs, but not that of any other individual HAT, leads to rapid and lethal autoimmunity (Xiao et al., 2014). In the absence of their acetylation, multiple lysines of Foxp3 can be ubiquitinated and lead to proteasomal degradation of Foxp3 protein (van Loosdregt et al., 2010). We previously noted that both Foxp3 and Tip60 in Tregs

were subject to proteasomal degradation (Xiao et al., 2014), but did not dissect the regulatory mechanisms. The current study now shows a major role for a single DUB, Usp7, in determining the fate of Foxp3 and Tip60 in Treg cells, thereby providing a target for therapeutic modulation of Treg function in the context of anti-tumor therapy.

Given the importance of Foxp3 and TIP60 in Treg biology, it is not surprising that regulatory mechanisms exist to limit their proteasomal turnover. In mammals, ~100 DUBs that hydrolyze the isopeptide bond
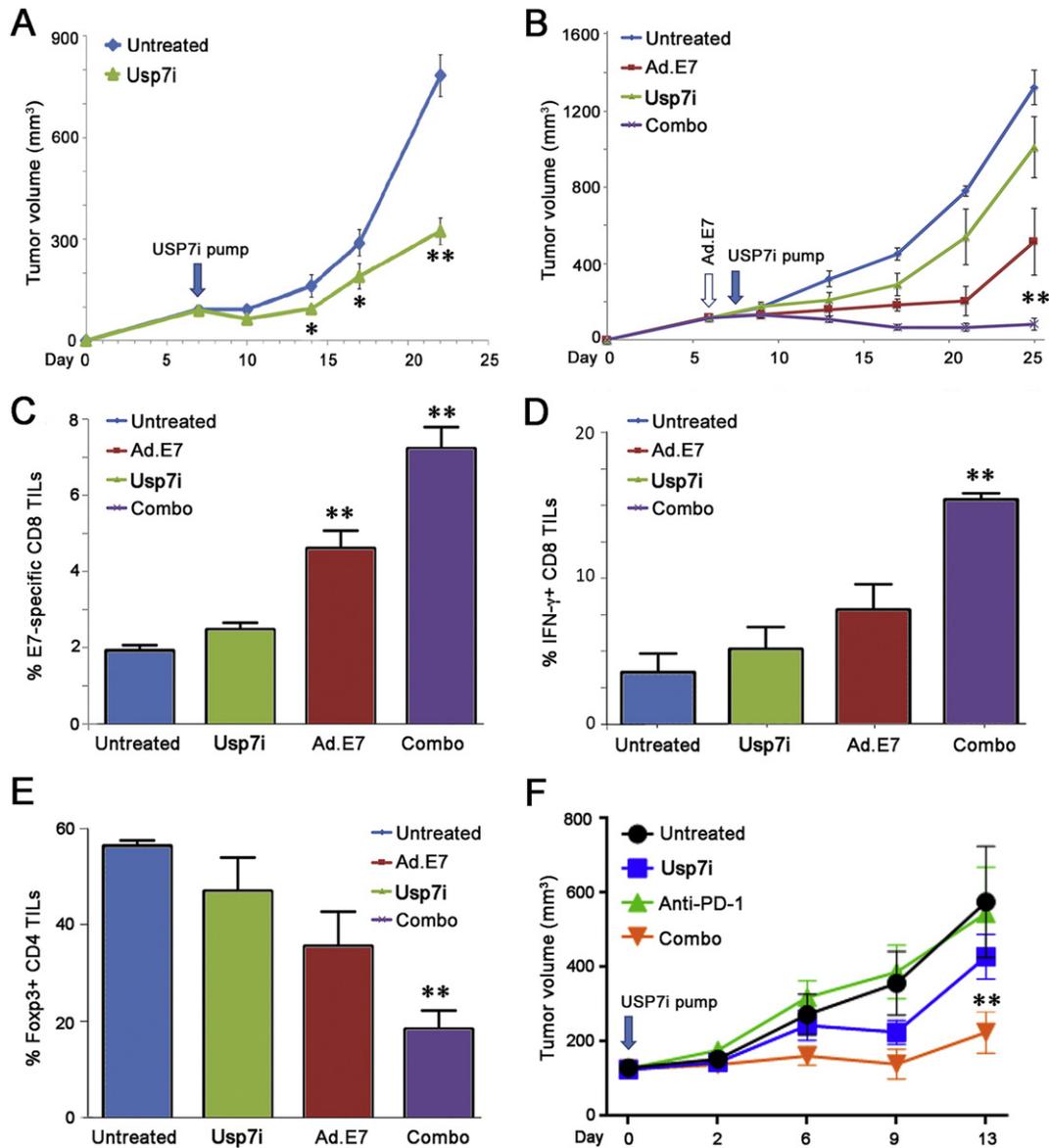
Fig. 6. Additional effects and combination therapies involving USP7i administration. (A) Effects of Usp7i therapy on the growth of AE.17 tumor cells in vivo. Usp7i therapy (6 mg/kg/day) decreased the growth of AE.17 tumor cells in syngeneic WT C57BL/6 mice (**p < 0.01); mean ± SD, n = 8–10 mice/group. (B) Six days after s.c. injection of TC1 cells, mice were injected with Ad.E7 (10^9 pfu) and 2 days later pumps delivering Usp7i (1 mg/kg/day) were inserted; panel (mean ± SEM) shows serial monitoring of tumor volumes in mice (10/group) that were either untreated, or received Ad.E7 or Usp7i alone, or their combination. Panels C-E show effects of therapy, at 13 days post-Ad.E7 vaccination, including: (C) %tetramer + CD8 tumor infiltrating lymphocytes (TILs) (**p < 0.01 vs. untreated or Usp7i-treated groups); (D) % IFNγ + CD8 cells among all CD8 TILs (**p < 0.01 vs. other groups); and (E) % Foxp3 + CD4 T cells among all CD4 TILs (**p < 0.01 vs. other groups). (F) Combination therapy with anti-PD-1 mAb (5 mg/kg/4 days) and Usp7i (1 mg/kg/day) in mice bearing TC1 lung tumors; day 0 on the x-axis indicates when implanted tumor volumes had reached ~150 mm³ and therapy was begun; mean ± SD, 8 mice/group, **p < 0.01 vs. other groups.

between ubiquitin and target proteins are divided into cysteine proteases and metalloproteases (Reyes-Turcu et al., 2009). The cysteine proteases include ubiquitin C-terminal hydrolases, ubiquitin specific protease, ovarian tumor proteases, and Machado-Joseph domain proteases, whereas the sole metalloprotease group comprises several Jab1/Mpn/Mov34 domain proteases. DUBs typically have a catalytic domain and several accessory domains that facilitate target interaction, protein-protein interactions, cell localization and other actions. Of the >50 mammalian USPs (Reyes-Turcu et al., 2009), some 21 USPs were detected in human Tregs and identified by ChIP studies as possible targets of FOXP3 (Sadlon et al., 2010). We focused on Usp7 for several reasons, including a report of Usp7 regulating Foxp3 expression in murine Treg cells (van Loosdregt et al., 2013). However, that study used a DUBi small molecule, that unlike compounds P5091 or 564, has several hundred fold greater potency against Usp8 vs. Usp7 (Colombo et al., 2010). Critically, Usp8 is well-expressed in Foxp3 + Treg cells

(http://www.ncbi.nlm.nih.gov/geoprofiles/?term=usp8+AND+Foxp3), and can stabilize expression of Ndrp1/RNF41 that is important to cytokine receptor (e.g. IL-2R) and retinoic acid receptor signaling (3–5), and vital for Foxp3 stabilization in thymic and/or induced Tregs (De Ceuninck et al., 2013; Jing et al., 2008; Wu et al., 2004).

In contrast, the current study used highly specific Usp7i small molecules, as well as conditional gene deletion, to definitively evaluate the effects of Usp7 targeting on host immune responses, including in the context of immuno-oncology. Our work does indicate a role for Usp7 in regulating Foxp3, but also identifies a potentially even more important action in regulating Tip60 in Treg cells. Usp7 can deubiquitinate and stabilize expression of Tip60 in transfected 293T cells (Dar et al., 2013) and in cultured 3T3-L1 adipocytes (Gao et al., 2013), indicating the potential for Usp7 to regulate the actions of Tip60 in non-hemopoietic cells. However, the current study highlights the role of Usp7 in regulation of Tip60 in Treg cells, as illustrated in schematic form in Fig. 7.
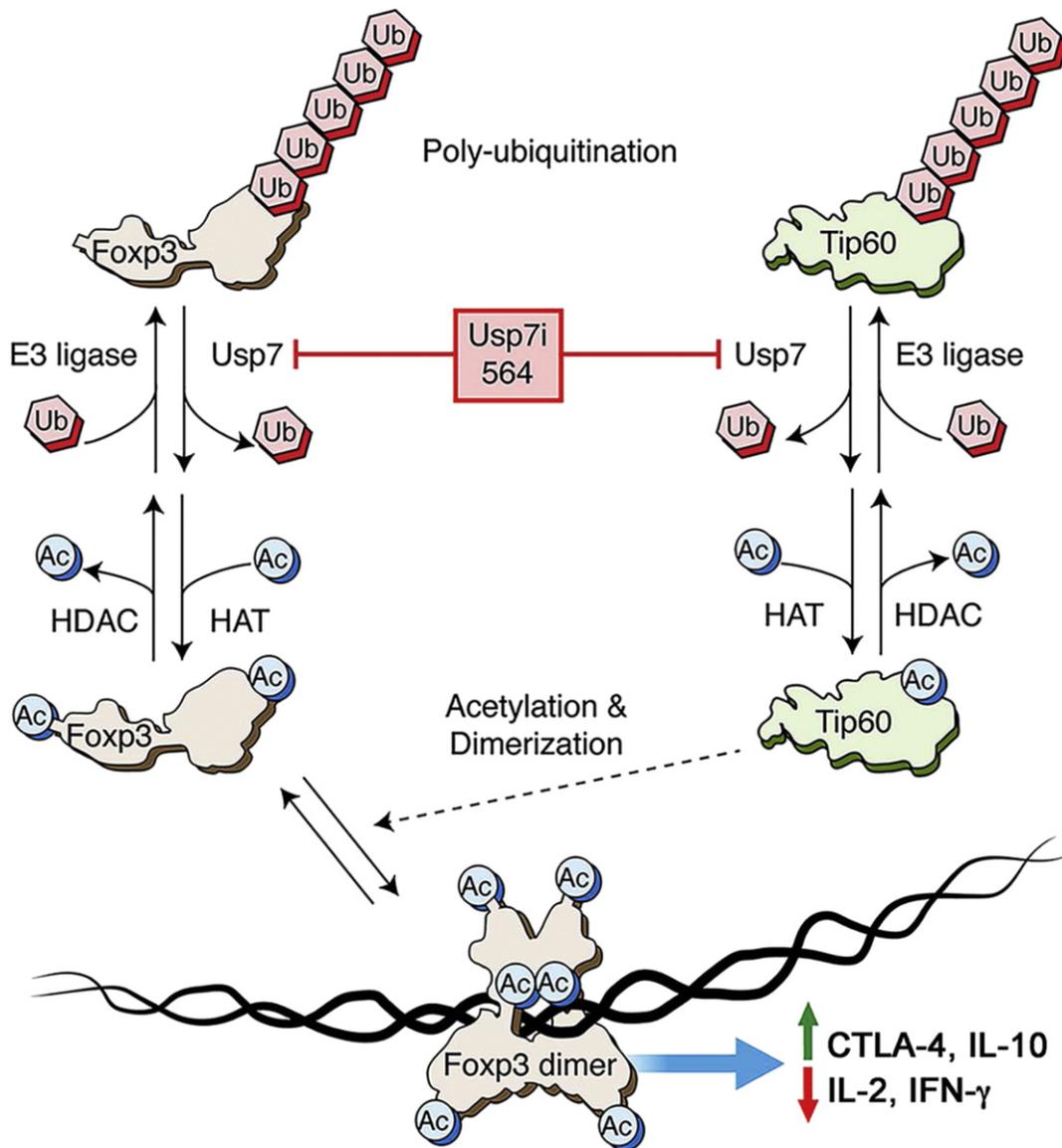
Fig. 7. Schematic of proposed interaction of Usp7i with Foxp3 + Treg cells. Lysine residues in both Foxp3 and Tip60 in Treg cells are subject to polyubiquitination, leading to protein turnover via their proteasomal degradation. Through the actions of Usp7, deubiquitinated lysine residues can be acetylated, leading to protein stabilization. While multiple HATs can acetylate Foxp3, Tip60, which can auto-acetylate, is unique in mediating acetylation of 2 lysine residues required for Foxp3 dimerization. Dimerized Foxp3 can then bind to DNA and mediate effects on gene transcription in Treg cells (e.g. upregulation of genes encoding Ctla4 and IL-10 and inhibition of genes encoding IL-2 and IFN-γ).

Usp7 is present in many, perhaps all cells, and its inhibition would be anticipated to promote the ubiquitination and proteasomal degradation of many cell proteins. However, the exquisite specificity of Foxp3 for Treg cells, and the key role of Tip60 in promoting Foxp3 dimerization, provides a mechanism by which Usp7i compounds can have dominant effects on Foxp3 + Tregs over that of other immune cell types, including host Teff cells. Likewise, within Treg cells, the requirement of Tip60-mediated acetylation for Foxp3 dimerization and Treg function makes this Usp7-regulated pathway a critical target for pharmacologic modulation of Treg cells using Usp7i compounds.

Usp7 is thought to exist in equilibrium between inactive and active forms, and its activity is enhanced allosterically by the metabolic enzyme, GMPS, which binds and activates the HUBL domain of Usp7, increasing the ubiquitin binding and catalytic activity of Usp7 by 100-fold (Faesen et al., 2011). Although details of the regulation of Usp7 activity in Tregs are still incomplete, our Usp7i data indicate that the catalytic site is important for the functions of Usp7 in Treg cells. Whether an additional scaffolding or adaptor function of Usp7 can play an important role in

Treg cells, e.g. by contributing to the assembly of large molecular complexes, remains to be determined.

The effects of Usp7 targeting on Foxp3 + Treg biology in our studies were profound and multifaceted. While both Foxp3 transcription and translation appeared unimpaired under basal conditions, Foxp3-dependent Treg functions were disrupted. An example of this dysfunction involved Treg production of IL-2. A defining characteristic of normal Foxp3 + Treg cells is their dependence upon IL-2 production by adjacent T cells for their survival (Fontenot et al., 2005; Gavin et al., 2007). This is due to Foxp3 binding to the IL-2 promoter in Tregs and inhibiting IL-2 expression. Our ChIP studies confirmed decreased binding of Foxp3 to the IL-2 promoter of Usp7-targeted Tregs, along with their production of IL-2 and other normally repressed cytokines. This failure to suppress IL-2, despite production of Foxp3 mRNA and protein, became explicable once the inhibitory effects of Usp7 targeting on Foxp3 dimerization and oligomerization were detected. Likewise, the more rapid and greater effects of Usp7 targeting on Tip60 vs. Foxp3 ubiquitination and turnover are consistent with a key role for regulation of Tip60

expression by Usp7 in Treg cells. Without normal levels of Tiop60 in Treg cells, Foxp3 dimerization and DNA binding is impaired and Treg function abrogated, despite ongoing Foxp3 mRNA and protein production. These effects of Usp7 on post-translational pathways in Tregs provide an important new insight of potential significance in anti-cancer therapy.

The ability of Usp7 targeting to selectively diminish Treg function has practical significance in cancer therapy, given the availability of highly specific and potent Usp7i compounds. Though initially identified as a protein associated with herpes simplex virus, Usp7 became widely known as its role in regulation of the p53 pathway was characterized (36, 37). Usp7 deubiquitinates Mdm2 and enhances its E3 ligase activity towards p53 protein, though p53-independent actions are recognized (Nicholson and Suresh Kumar, 2011). Hence, inhibition of Usp7 is thought to inactivate Mdm2 and thereby activate p53, resulting in inhibition of cell cycle progression and tumor cell apoptosis. In the current studies, the negligible direct effects of Usp7i administration on tumor growth in vivo are consistent with the low levels of p53 and Mdm2 in the tumors employed in our studies, and contrast with a previous study in which compound P5091 had direct effects on the growth of human multiple myeloma cells as xenografts in immunodeficient mice (Chauhan et al., 2012). Levels of p53 and Hdm2, the human counterpart of Mdm2, were considerably higher in those myeloma cells than in TC1 or AE.17 cells (Fig. S19). Levels of p53 were also low in murine Tregs, with or without *Usp7* deletion, such that the effects of Usp7i on tumor growth in immunocompetent hosts likely reflect disruption of Treg function, via effects on Tip60 and Foxp3, than via a p53-dominant mechanism. The increased resistance of Usp7i-treated Teff cells to Treg suppression is an additional therapeutic mechanism resistance of Usp7i-treated Teff cells to suppression by untreated WT Tregs ($p < 0.05$) (Fig. 4B, Fig. S15), albeit as yet unexplored. However, it is to be expected that in some tumor models in syngeneic hosts, the effects of Usp7i administration will include direct anti-tumor effects as well as immune actions, and the relative contributions of these mechanisms may differ. In either situation, increased anti-tumor activity would be expected.

The current data also show that Usp7i therapy, likely via its inhibitory effects on Tregs, can potentiate the effects of antitumor vaccination, PD-1 targeting, and other immunotherapies in experimental models. This may increase the efficacy of a given approach, allow reduced intensity of therapy with a single agent, and reduce development of resistance as a result of multiple mechanisms of action. Hence, the further development and clinical testing of Usp7i compounds appears a logical and potentially valuable new approach in the immunotherapy of cancer.

Conflict of Interest Statement

Suresh Kumar, Feng Wang, Jian Wu, Benjamin Nicholson, Mathew P. Kodrasov, Saket Agarwal, David E. Sterner, Joseph Weinstock, and Tauseef R. Butt are employees of Progenra, Inc., developers of the Usp7i compounds utilized in this paper.

Author Contributions

L.W. performed the Treg studies, analyzed data and edited the manuscript. S.K., F.W., J. Wu, B.N., M.P.K., S.A. D.E.S., J. Weinstock and T.R.B. generated Usp7i compounds and undertook biochemical studies. S.D. and A.S. contributed and analyzed data. K.N. and S.M.A. performed tumor studies and analyzed tumor data. R.H. undertook mouse breeding and performed histology. U.H.B. analyzed microarray data, analyzed data and edited the manuscript. T.R.B. performed histology. T.A. performed autoantibody screening, analyzed data and edited the manuscript. W.G. provided unique mice and analyzed data. W.W.H. designed and directed this study, analyzed data and wrote the manuscript.

Appendix A. Supplementary data

Supplementary data to this article can be found online at doi:10. 1016/j.ebiom.2016.10.018.

References

American_Cancer_Society, 2015. Cancer Facts and Figures. In American Cancer Society 2015.

Antony, P.A., Piccirillo, C.A., Akpinarli, A., Finkelstein, S.E., Speiss, P.J., Surman, D.R., Palmer, D.C., Chan, C.C., Klebanoff, C.A., Overwijk, W.W., et al., 2005. CD8 + T cell immunity against a tumor/self-antigen is augmented by CD4 + T helper cells and hindered by naturally occurring T regulatory cells. J. Immunol. 174, 2591–2601.

Attia, P., Maker, A.V., Haworth, L.R., Rogers-Freezer, L., Rosenberg, S.A., 2005. Inability of a fusion protein of IL-2 and diphtheria toxin (Denileukin Diftitox, DAB389IL-2, ONTAK) to eliminate regulatory T lymphocytes in patients with melanoma. J. Immunother. 28, 582–592.

Battke, F., Symons, S., Nieselt, K., 2010. Mayday–integrative analytics for expression data. BMC Biotechnol. 11, 121.

Beyer, M., Schultze, J.L., 2006. Regulatory T cells in cancer. Blood 108, 804–811.

Boudreaux, D.A., Maiti, T.K., Davies, C.W., Das, C., 2010. Ubiquitin vinyl methyl ester binding orients the misaligned active site of the ubiquitin hydrolase UCHL1 into productive conformation. Proc. Natl. Acad. Sci. U. S. A. 107, 9117–9122.

Brahmer, J.R., Tykodi, S.S., Chow, L.Q., Hwu, W.J., Topalian, S.L., Hwu, P., Drake, C.G., Camacho, L.H., Kauh, J., Odunsi, K., et al., 2012. Safety and activity of anti-PD-L1 antibody in patients with advanced cancer. N. Engl. J. Med. 366, 2455–2465.

Chauhan, D., Tian, Z., Nicholson, B., Kumar, K.G., Zhou, B., Carrasco, R., McDermott, J.L., Leach, C.A., Fulcinniti, M., Kodrasov, M.P., et al., 2012. A small molecule inhibitor of ubiquitin-specific protease-7 induces apoptosis in multiple myeloma cells and overcomes bortezomib resistance. Cancer Cell 22, 345–358.

Colombo, M., Vallese, S., Peretto, I., Jacq, X., Rain, J.C., Colland, F., Guedat, P., 2010. Synthesis and biological evaluation of 9-oxo-9H-indeno[1,2-b]pyrazine-2,3-dicarbonitrile analogues as potential inhibitors of deubiquitinating enzymes. ChemMedChem 5, 552–558.

Cummins, J.M., Rago, C., Kohli, M., Kinzler, K.W., Lengauer, C., Vogelstein, B., 2004. Tumour suppression: disruption of HAUSP gene stabilizes. Nature 428, 53 (1 p following 486).

Curiel, T.J., 2007. Tregs and rethinking cancer immunotherapy. J. Clin. Invest. 117, 1167–1174.

Dar, A., Shibata, E., Dutta, A., 2013. Deubiquitination of Tip60 by USP7 determines the activity of the p53-dependent apoptotic pathway. Mol. Cell. Biol. 33, 3309–3320.

De Ceuninck, L., Wauman, J., Masschaele, D., Peelman, F., Tavernier, J., 2013. Reciprocal cross-regulation between RNF41 and USP8 controls cytokine receptor sorting and processing. J. Cell Sci. 126, 3770–3781.

Dougan, M., Dranoff, G., 2009. Immune therapy for cancer. Annu. Rev. Immunol. 27, 83–117.

Dranoff, G., 2005. CTLA-4 blockade: unveiling immune regulation. J. Clin. Oncol. 23, 662–664.

Du, T., Nagai, Y., Xiao, Y., Greene, M.I., Zhang, H., 2013. Lysosome-dependent p300/FOXP3 degradation and limits Treg cell functions and enhances targeted therapy against cancers. Exp. Mol. Pathol. 95, 38–45.

Dyck, L., Wilk, M.M., Raverdeau, M., Misiak, A., Boon, L., Mills, K.H., 2016. Anti-PD-1 inhibits Foxp3 + Treg cell conversion and unleashes intratumoural effector T cells thereby enhancing the efficacy of a cancer vaccine in a mouse model. Cancer Immunol. Immunother. http://dx.doi.org/10.1007/s00262-016-1906-6 (in press).

Faesen, A.C., Dirac, A.M., Shanmugham, A., Ovaa, H., Perrakis, A., Sixma, T.K., 2011. Mechanism of USP7/HAUSP activation by its C-terminal ubiquitin-like domain and allosteric regulation by GMP-synthetase. Mol. Cell 44, 147–159.

Fietta, A.M., Morosini, M., Passadore, I., Cascina, A., Draghi, P., Dore, R., Rossi, S., Pozzi, E., Meloni, F., 2009. Systemic inflammatory response and downmodulation of peripheral CD25 + Foxp3 + T-regulatory cells in patients undergoing radiofrequency thermal ablation for lung cancer. Hum. Immunol. 70, 477–486.

Fontenot, J.D., Rasmussen, J.P., Gavin, M.A., Rudensky, A.Y., 2005. A function for interleukin 2 in Foxp3-expressing regulatory T cells. Nat. Immunol. 6, 1142–1151.

Fu, W., Ergun, A., Lu, T., Hill, J.A., Haxhinasto, S., Fassett, M.S., Gazit, R., Adoro, S., Glimcher, L., Chan, S., et al., 2012. A multiply redundant genetic switch 'locks in' the transcriptional signature of regulatory T cells. Nat. Immunol. 13, 972–980.

Gallimore, A., Godkin, A., 2008. Regulatory T cells and tumour immunity - observations in mice and men. Immunology 123, 157–163.

Gallimore, A.M., Simon, A.K., 2008. Positive and negative influences of regulatory T cells on tumour immunity. Oncogene 27, 5886–5893.

Gao, Y., Koppen, A., Rakhshandehroo, M., Tasdelen, I., van de Graaf, S.F., van Loosdregt, J., van Beekum, O., Hamers, N., van Leenen, D., Berkers, C.R., et al., 2013. Early adipogenesis is regulated through USP7-mediated deubiquitination of the histone acetyltransferase TIP60. Nat. Commun. 4, 2656.

Gavin, M.A., Rasmussen, J.P., Fontenot, J.D., Vasta, V., Manganiello, V.C., Beavo, J.A., Rudensky, A.Y., 2007. Foxp3-dependent programme of regulatory T-cell differentiation. Nature 445, 771–775.

Ha, T.Y., 2009. The role of regulatory T cells in cancer. Immune Netw 9, 209–235.

Haas, A.R., Sun, J., Vachani, A., Wallace, A.F., Silverberg, M., Kapoor, V., Albelda, S.M., 2006. Cycloxygenase-2 inhibition augments the efficacy of a cancer vaccine. Clin. Cancer Res. 12, 214–222.

Hanahan, D., Weinberg, R.A., 2000. The hallmarks of cancer. Cell 100, 57–70.

Hancock, W.W., Buelow, R., Sayegh, M.H., Turka, L.A., 1998. Antibody-induced transplant arteriosclerosis is prevented by graft expression of anti-oxidant and anti-apoptotic genes. Nat. Med. 4, 1392–1396.

Huang da, W., Sherman, B.T., Lempicki, R.A., 2009. Systematic and integrative analysis of large gene lists using DAVID bioinformatics resources. Nat. Protoc. 4, 44–57.

Jackaman, C., Bundell, C.S., Kinnear, B.F., Smith, A.M., Filion, P., van Hagen, D., Robinson, B.W., Nelson, D.J., 2003. IL-2 intratumoral immunotherapy enhances CD8 + T cells that mediate destruction of tumor cells and tumor-associated vasculature: a novel mechanism for IL-2. J. Immunol. 171, 5051–5063.

Jing, X., Infante, J., Nachtman, R.G., Jurecic, R., 2008. E3 ligase FLRF (Rnf41) regulates differentiation of hematopoietic progenitors by governing steady-state levels of cytokine and retinoic acid receptors. Exp. Hematol. 36, 1110–1120.

Ke, X., Wang, J., Li, L., Chen, I.H., Wang, H., Yang, X.F., 2008. Roles of CD4 + CD25(high) FOXP3 + Tregs in lymphomas and tumors are complex. Front. Biosci. 13, 3986–4001.

Knutson, K.L., Dang, Y., Lu, H., Lukas, J., Almand, B., Gad, E., Azeke, E., Disis, M.L., 2006. IL-2 immunotoxin therapy modulates tumor-associated regulatory T cells and leads to lasting immune-mediated rejection of breast cancers in neu-transgenic mice. J. Immunol. 177, 84–91.

Kon, N., Zhong, J., Kobayashi, Y., Li, M., Szabolcs, M., Ludwig, T., Canoll, P.D., Gu, W., 2011. Roles of HAUSP-mediated p53 regulation in central nervous system development. Cell Death Differ. 18, 1366–1375.

Lee, P.P., Fitzpatrick, D.R., Beard, C., Jessup, H.K., Lehar, S., Makar, K.W., Perez-Melgosa, M., Sweetser, M.T., Schlissel, M.S., Nguyen, S., et al., 2001. A critical role for Dnmt1 and DNA methylation in T cell development, function, and survival. Immunity 15, 763–774.

Lee, I., Wang, L., Wells, A.D., Dorf, M.E., Ozkaynak, E., Hancock, W.W., 2005. Recruitment of Foxp3 + T regulatory cells mediating allograft tolerance depends on the CCR4 chemokine receptor. J. Exp. Med. 201, 1037–1044.

Li, M., Brooks, C.L., Kon, N., Gu, W., 2004. A dynamic role of HAUSP in the p53-Mdm2 pathway. Mol. Cell 13, 879–886.

Li, B., Samanta, A., Song, X., Iacono, K.T., Bembas, K., Tao, R., Basu, S., Riley, J.L., Hancock, W.W., Shen, Y., et al., 2007. FOXP3 interactions with histone acetyltransferase and class II histone deacetylases are required for repression. Proc. Natl. Acad. Sci. U. S. A. 104, 4571–4576.

Lin, K.Y., Guarnieri, F.G., Staveley-O'Carroll, K.F., Levitsky, H.I., August, J.T., Pardoll, D.M., Wu, T.C., 1996. Treatment of established tumors with a novel vaccine that enhances major histocompatibility class II presentation of tumor antigen. Cancer Res. 56, 21–26.

Liu, Y., Wang, L., Han, R., Beier, U.H., Hancock, W.W., 2012. Two lysines in the forkhead domain of foxp3 are key to T regulatory cell function. PLoS One 7, e29035.

Liu, Y., Wang, L., Predina, J., Han, R., Beier, U.H., Wang, L.C., Kapoor, V., Bhatti, T.R., Akimova, T., Singhal, S., et al., 2013. Inhibition of p300 impairs Foxp3 + T regulatory cell function and promotes antitumor immunity. Nat. Med. 19, 1173–1177.

Liu, Y., Wang, L., Han, R., Beier, U.H., Akimova, T., Bhatti, T., Xiao, H., Cole, P.A., Brindle, P.K., Hancock, W.W., 2014. Two histone/protein acetyltransferases, CBP and p300, are indispensable for Foxp3 + T-regulatory cell development and function. Mol. Cell. Biol. 34, 3993–4007.

Nicholson, B., Suresh Kumar, K.G., 2011. The multifaceted roles of USP7: new therapeutic opportunities. Cell Biochem. Biophys. 60, 61–68.

Nishikawa, H., Sakaguchi, S., 2010. Regulatory T cells in tumor immunity. Int. J. Cancer 127, 759–767.

O'Callaghan, D.S., Rexhepaj, E., Gately, K., Coate, L., Delaney, D., O'Donnell, D.M., Kay, E., O'Connell, F., Gallagher, W.M., O'Byrne, K.J., 2015. Tumour islet Foxp3 + T-cell infiltration predicts poor outcome in nonsmall cell lung cancer. Eur Respir J 46, 1762–1772.

Pardoll, D.M., 2012. The blockade of immune checkpoints in cancer immunotherapy. Nat. Rev. Cancer 12, 252–264.

Petersen, R.P., Campa, M.J., Sperlazza, J., Conlon, D., Joshi, M.B., Harpole Jr., D.H., Patz Jr., E.F., 2006. Tumor infiltrating Foxp3 + regulatory T-cells are associated with recurrence in pathologic stage I NSCLC patients. Cancer 107, 2866–2872.

Powell Jr., D.J., Felipe-Silva, A., Merino, M.J., Ahmadzadeh, M., Allen, T., Levy, C., White, D.E., Mavroukakis, S., Kreitman, R.J., Rosenberg, S.A., et al., 2007. Administration of a CD25-directed immunotoxin, LMB-2, to patients with metastatic melanoma induces a selective partial reduction in regulatory T cells in vivo. J. Immunol. 179, 4919–4928.

Qin, F.X., 2009. Dynamic behavior and function of Foxp3 + regulatory T cells in tumor bearing host. Cell. Mol. Immunol. 6, 3–13.

Reyes-Turcu, F.E., Ventii, K.H., Wilkinson, K.D., 2009. Regulation and cellular roles of ubiquitin-specific deubiquitinating enzymes. Annu. Rev. Biochem. 78, 363–397.

Roth, S.Y., Denu, J.M., Allis, C.D., 2001. Histone acetyltransferases. Annu. Rev. Biochem. 70, 81–120.

Rubtsov, Y.P., Rasmussen, J.P., Chi, E.Y., Fontenot, J., Castelli, L., Ye, X., Treuting, P., Siewe, L., Roers, A., Henderson Jr., W.R., et al., 2008. Regulatory T cell-derived interleukin-10 limits inflammation at environmental interfaces. Immunity 28, 546–558.

Rubtsov, Y.P., Niec, R.E., Josefowicz, S., Li, L., Darce, J., Mathis, D., Benoist, C., Rudensky, A.Y., 2010. Stability of the regulatory T cell lineage in vivo. Science 329, 1667–1671.

Rudra, D., deRoos, P., Chaudhry, A., Niec, R.E., Arvey, A., Samstein, R.M., Leslie, C., Shaffer, S.A., Goodlett, D.R., Rudensky, A.Y., 2012. Transcription factor Foxp3 and its protein partners form a complex regulatory network. Nat. Immunol. 13, 1010–1019.

Sadlon, T.J., Wilkinson, B.G., Pederson, S., Brown, C.Y., Bresatz, S., Gargett, T., Melville, E.L., Peng, K., D'Andrea, R.J., Glonek, G.G., et al., 2010. Genome-wide identification of human FOXP3 target genes in natural regulatory T cells. J. Immunol. 185, 1071–1081.

Sharma, P., Wagner, K., Wolchok, J.D., Allison, J.P., 2011. Novel cancer immunotherapy agents with survival benefit: recent successes and next steps. Nat. Rev. Cancer 11, 805–812.

Song, X., Li, B., Xiao, Y., Chen, C., Wang, Q., Liu, Y., Berezov, A., Xu, C., Gao, Y., Li, Z., et al., 2012. Structural and biological features of FOXP3 dimerization relevant to regulatory T cell function. Cell Rep. 1, 665–675.

Tao, R., de Zoeten, E.F., Ozkaynak, E., Chen, C., Wang, L., Porrett, P.M., Li, B., Turka, L.A., Olson, E.N., Greene, M.I., et al., 2007. Deacetylase inhibition promotes the generation and function of regulatory T cells. Nat. Med. 13, 1299–1307.

Topalian, S.L., Hodi, F.S., Brahmer, J.R., Gettinger, S.N., Smith, D.C., McDermott, D.F., Powderly, J.D., Carvajal, R.D., Sosman, J.A., Atkins, M.B., et al., 2012. Safety, activity, and immune correlates of anti-PD-1 antibody in cancer. N. Engl. J. Med. 366, 2443–2454.

van Loosdregt, J., Vercoulen, Y., Guichelaar, T., Gent, Y.Y., Beekman, J.M., van Beekum, O., Brenkman, A.B., Hijnen, D.J., Mutis, T., Kalkhoven, E., et al., 2010. Regulation of Treg functionality by acetylation-mediated Foxp3 protein stabilization. Blood 115, 965–974.

van Loosdregt, J., Fleskens, V., Fu, J., Brenkman, A.B., Bekker, C.P., Pals, C.E., Meerding, J., Berkers, C.R., Barbi, J., Grone, A., et al., 2013. Stabilization of the transcription factor Foxp3 by the deubiquitinase USP7 increases Treg-cell-suppressive capacity. Immunity 39, 259–271.

Wang, L., Liu, Y., Han, R., Beier, U.H., Bhatti, T.R., Akimova, T., Greene, M.I., Hiebert, S.W., Hancock, W.W., 2015. FOXP3 + regulatory T cell development and function require histone/protein deacetylase 3. J. Clin. Invest. 125, 1111–1123.

Weinstock, J., Wu, J., Cao, P., Kingsbury, W.D., McDermott, J.L., Kodrasov, M.P., McKelvey, D.M., Suresh Kumar, K.G., Goldenberg, S.J., Mattern, M.R., et al., 2012. Selective dual inhibitors of the cancer-related Deubiquitylating proteases USP7 and USP47. ACS Med. Chem. Lett. 3, 789–792.

Woo, E.Y., Chu, C.S., Goletz, T.J., Schlienger, K., Yeh, H., Coukos, G., Rubin, S.C., Kaiser, L.R., June, C.H., 2001. Regulatory CD4(+)CD25(+) T cells in tumors from patients with early-stage non-small cell lung cancer and late-stage ovarian cancer. Cancer Res. 61, 4766–4772.

Wu, X., Yen, L., Irwin, L., Sweeney, C., Carraway 3rd, K.L., 2004. Stabilization of the E3 ubiquitin ligase Nrdp1 by the deubiquitinating enzyme USP8. Mol. Cell. Biol. 24, 7748–7757.

Xiao, Y., Nagai, Y., Deng, G., Ohtani, T., Zhu, Z., Zhou, Z., Zhang, H., Ji, M.Q., Lough, J.W., Samanta, A., et al., 2014. Dynamic interactions between TIP60 and p300 regulate FOXP3 function through a structural switch defined by a single lysine on TIP60. Cell Rep. 7, 1471–1480.

Yang, H.Y., Barbi, J., Wu, C.Y., Zheng, Y., Vignali, P.D., Wu, X., Tao, J.H., Park, B.V., Bandara, S., Novack, L., et al., 2016. MicroRNA-17 modulates regulatory T cell function by targeting Co-regulators of the Foxp3 transcription factor. Immunity 45, 83–93.

Zheng, Y., Josefowicz, S., Chaudhry, A., Peng, X.P., Forbush, K., Rudensky, A.Y., 2010. Role of conserved non-coding DNA elements in the Foxp3 gene in regulatory T-cell fate. Nature 463, 808–812.

Zitvogel, L., Tesniere, A., Kroemer, G., 2006. Cancer despite immunosurveillance: immunoselection and immunosubversion. Nat. Rev. Immunol. 6, 715–727.

Zitvogel, L., Apetoh, L., Ghiringhelli, F., Andre, F., Tesniere, A., Kroemer, G., 2008. The anticancer immune response: indispensable for therapeutic success? J. Clin. Invest. 118, 1991–2001.